Journal of Nuclear Materials 430 (2012) 90–95

Contents lists available at SciVerse ScienceDirect

Journal of Nuclear Materials

journal homepage: www.elsevier.com/locate/jnucmat

Mechanics of a crushable pebble assembly using discrete element method

R.K. Annabattula [a,*], Y. Gan [b], S. Zhao [c], M. Kamlah [a]

[a] Institute for Applied Materials (IAM-WBM), Karlsruhe Institute of Technology (KIT), D-76344 Eggenstein-Leopoldshafen, Germany
[b] School of Civil Engineering, The University of Sydney, 2006 NSW, Sydney, Australia
[c] College of Mechanical and Electronics Engineering, Hebei University of Science and Technology, Shijiazhuang, Hebei 050018, China

ARTICLE INFO

Article history:
Received 2 May 2012
Accepted 27 June 2012
Available online 7 July 2012

ABSTRACT

The influence of crushing of individual pebbles on the overall strength of a pebble assembly is investigated using discrete element method. An assembly comprising of 5000 spherical pebbles is assigned with random critical failure energies with a Weibull distribution in accordance with the experimental observation. Then, the pebble assembly is subjected to uni-axial compression ($\epsilon_{33} = 1.5\%$) with periodic boundary conditions. The crushable pebble assembly shows a significant difference in stress–strain response in comparison to a non-crushable pebble assembly. The analysis shows that a ideal plasticity like behaviour (constant stress with increase in strain) is the characteristic of a crushable pebble assembly with sudden damage. The damage accumulation law plays a critical role in determining the critical stress while the critical number of completely failed pebbles at the onset of critical stress is independent of such a damage law. Furthermore, a loosely packed pebble assembly shows a higher crush resistance while the critical stress is insensitive to the packing factor (η) of the assembly.

1. Introduction

Breeder materials in the form of pebbles are used to breed tritium in helium cooled pebble beds (HCPBs) in fusion reactors [1]. The knowledge of crushing strength of individual pebbles and its influence on overall strength of the pebble assembly is important to ensure a safe and reliable operation of the solid breeder blankets in HCPB fusion reactors. The crushing strength of unirradiated Lithium Orthosilicate (Li_4SiO_4 or OSi) pebbles has been investigated both experimentally and numerically by Zhao [2]. A similar test for characterizing the crush strength of pebbles has been conducted in *Fusion Materials Laboratory at KIT* in an inert environment with BK7 glass as the plate material. Prior to conducting these crush experiments, the pebbles are conditioned by heating them at 300 °C for an hour. Fig. 1 shows the conditioned OSi pebbles between the crush plates, in a pebble bed and various forms of their failure observed in the experiments. The critical elastic strain energy (W_c) distribution of the Li_4SiO_4 pebbles has been shown to follow Weibull distribution from several crush tests, conform Fig. 2a. The probability distribution of critical failure energy can be fitted by [2,3]

$$P_s = 1 - \exp\left[-(12116W_c)^{3.17}\right]. \quad (1)$$

A large variation in the critical failure energy can be attributed to the presence of random impurities and variable porosity in the pebble material. Hence, it is important to consider an assembly of pebbles with varying pebble strength (critical energy for failure) in the numerical models to understand the mechanical behaviour of the pebble beds. In this paper, we investigate the influence of various damage criteria and packing factors on the macroscopic response of a pebble assembly. The outline of the paper is as follows. In Section 2, we present the model and the methodology used to incorporate the crush behaviour of the pebbles for DEM simulations. In Section 3, results of the simulations will be discussed. Finally, in Section 4 some concluding remarks based on our model and the results will be presented.

2. Model

In this work, we introduce a damage variable (D_i) analogous to continuum damage mechanics which evolves during loading as a function of normalized stored elastic energy of the pebble (ϕ_i/ϕ_i^{cr}). Pebble i starts to fail when the stored elastic energy (ϕ_i) exceeds the critical failure energy ($\phi_i^{cr} = W_c$). After the onset of failure, ceramic pebbles break into different pieces resulting in sudden vanishing of the contact forces in action. However, simulating the event of splitting of pebble into many pieces [4] is a complicated, unstable and computationally intensive task. Hence, in this paper we propose an alternative approach, i.e., reducing the elastic modulus of the pebble resembling the loss of load carrying capacity as a results of pebble crushing. In the present work, we

* Corresponding author. Tel.: + 49 72160825857; fax: +49 72160825859.
E-mail addresses: ratna.annabattula@kit.edu (R.K. Annabattula), yixiang.gan@sydney.edu.au (Y. Gan), marc.kamlah@kit.edu (M. Kamlah).

0022-3115/$ - see front matter © 2012 Elsevier B.V. All rights reserved.
http://dx.doi.org/10.1016/j.jnucmat.2012.06.043

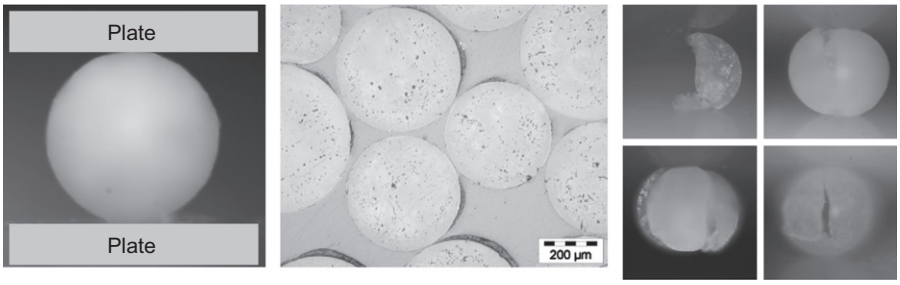

Fig. 1. OSi pebble between crush plates (left), conditioned OSi pebbles in a pebble bed (centre) and various failure forms of pebbles (right).

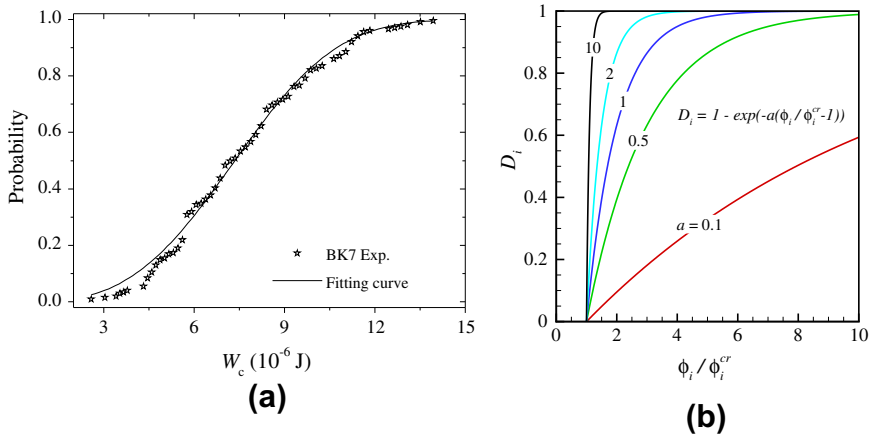

Fig. 2. (a) Probability distribution of critical elastic strain energy of conditioned OSi pebbles in a crush test with BK7 glass in an inert gas environment. (b) Damage law used for the accumulation of damage inside the pebble as a function of normalized stored elastic strain energy.

reduce the elastic modulus of the pebble as a function of its damage level (D_i) according to $E_i = (1 - D_i)E_0$, where E_0 = 90 GPa is the initial elastic modulus of the pebble materials [5].

The elastic energy stored in a pebble (ϕ_i) is calculated by the contact forces exerted on the pebble due to contact with the neighbouring pebbles using Hertzian theory. The value of the damage variable $D_i = 0$ until the stored elastic energy ϕ_i in the pebble is less than the critical failure energy ϕ_i^{cr}. The damage value D_i starts to increase (for $\phi_i/\phi_i^{cr} > 1$) according to

$$D_i = 1 - \exp\left(-a\left(\frac{\phi_i}{\phi_i^{cr}} - 1\right)\right), \tag{2}$$

where a is the coefficient of the damage evolution. Evolution of the damage variable D_i is shown in Fig. 2b for different values of a. The coefficient a describes the rate at which D_i approaches unity from the onset of failure (i.e., from $\phi_i/\phi_i^{cr} = 1$). In other words, large values of a indicate brittle failure (e.g., $a = 10$ in Fig. 2b) while small values resemble gradual failure (e.g., $a < 1$ in Fig. 2b). The gradual failure describes that, after the crushing event, the fragments of the pebble may still carry further loads with the confined condition by its neighbouring pebbles. From the equation for the evolution of elastic modulus as a function of damage level, it can be deduced that the elastic modulus becomes zero as the damage variable D_i approaches unity. Hence, in the present analysis, we specify a lower limit of $1.11 \times 10^{-8} E_0$ for E for any pebble in the assembly during the damage accumulation to avoid numerical instabilities. Furthermore, the damage is considered to be irreversible, meaning that at time t if the damage for a particular pebble calculated from Eq. (2) is smaller than the value obtained in the previous time step, then the damage D_i is not reduced but retained at the previous value. A flow chart depicting the procedure employed for the calculation and update of the damage variable D_i is shown in Fig. 3a.

3. Results and discussion

Discrete element simulations using an in-house DEM code [6] have been carried out by incorporating the aforementioned damage criterion (see Figs. 2b and 3a). The model system is a pebble assembly (in a cubic box) consisting of 5000 spherical particles of diameter 0.5 mm with periodic boundary conditions and is subjected to uni-axial compression in z direction (see Fig. 3b). The granular assembly has been generated using a random close packing algorithm [7,8] showing a very good correspondence with the X-ray tomography measurements [8] of the pebble bed packings similar to the pebble bed assemblies studied in this paper. Simulations have been carried out using different damage coefficients (a) and packing factors (η). The pebble assembly is subjected to quasi-static loading of uni-axial compression up to a strain $\epsilon_{33} = 1.5\%$ followed by unloading to a stress free state $\sigma_{33} \approx 0$.

Fig. 4 shows the stress–strain response of a pebble assembly under the action of uni-axial compression for different damage criteria and packing factors. Fig. 4a shows the effect of different damage criteria on the overall stress–strain response of the pebble assembly. Here, the damage coefficient is varied from a no-damage condition (i.e., $a = 0$) through gradual damage condition ($a = 0.1, 0.5, 1$) to a sudden damage condition (a = 10). We can observe a clear dependence of the stress–strain behaviour on the damage criterion. The assembly with sudden damage criterion (a = 10) exhibits an initial non-linear elastic response followed by a ideal plasticity like behaviour and the stress at which this plateau continues is referred to as "critical stress" hereafter. In the case of

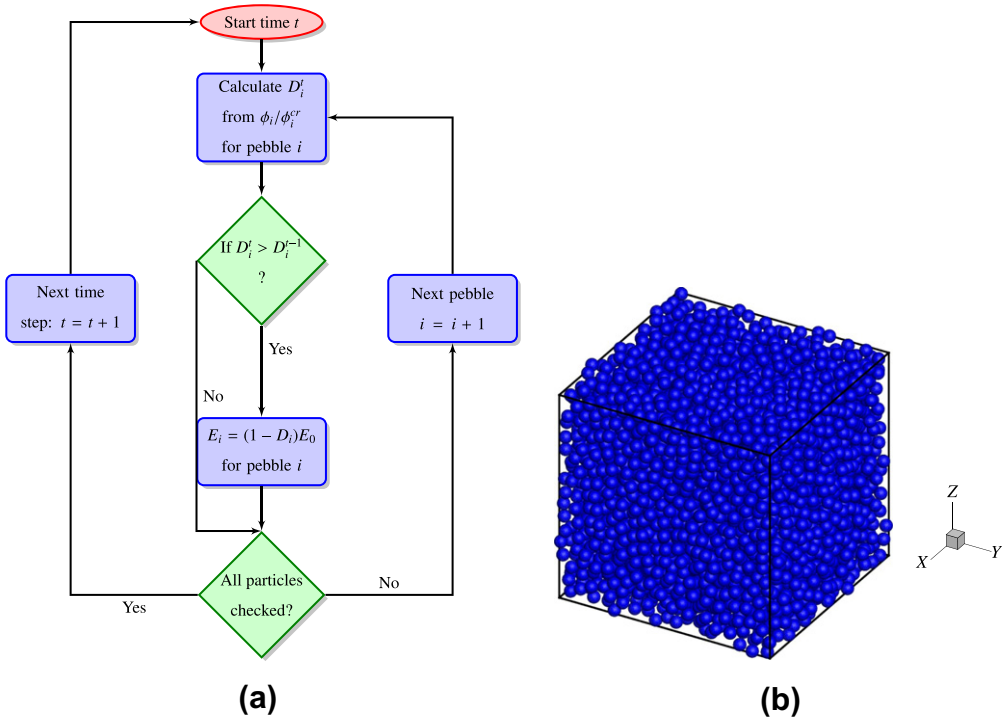

Fig. 3. (a) Flow chart showing the damage evaluation scheme. (b) Initial configuration of a pebble assembly showing zero damage in the pebbles.

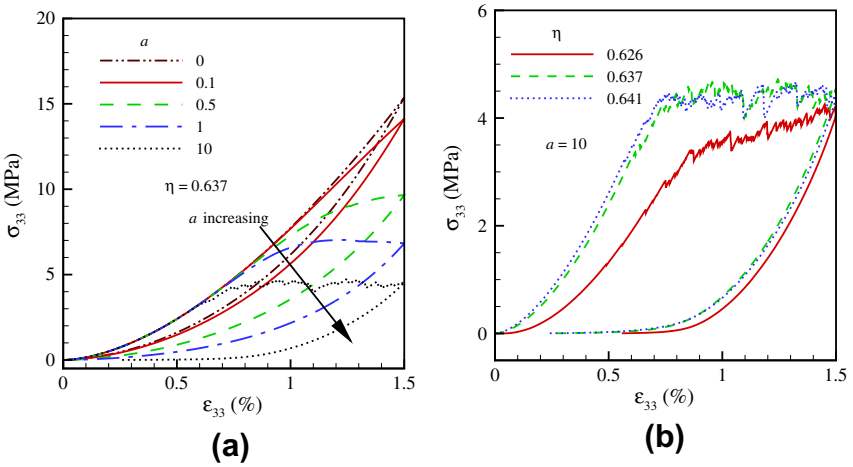

Fig. 4. Average stress vs strain for a pebble assembly (a) with a packing factor $\eta = 0.637$ for different damage criteria as shown in Fig. 2b (b) with a damage coefficient $a = 10$ and for different packing factors.

gradual damage ($a < 1$, in this paper), the critical stress increases with decrease in the value of a finally reaching the non-crushable pebble assembly ($a = 0$) response. Also note that the value of critical stress is less ambiguous in the case of sudden damage (large a) compared to gradual damage. The residual strain after unloading also depends on the value of damage coefficient a. If the value of the damage coefficient (a) is high, then the assembly is prone to more damage at the same strain level compared to a low value of a. Hence, after the loading step is completed, the assembly with large a value will be more compliant resulting in large residual strain after unloading as shown in Fig. 4a (compare dotted line with dashed-dotted line). For damage coefficient values larger than 10, the corresponding stress–strain curves in the loading stage coincide and the residual strain after unloading increases with increase in a. Also, note that the onset of critical stress occurs at same strain and the number of pebbles that fail completely (i.e., $D_i = 1$) at this critical strain is independent of damage coefficient a although the total number of damaged pebbles differ at the end of loading (for different values of damage coefficient $a > 10$) in the case of sudden damage [9]. Fig. 4b shows the effect of packing factor on the stress–strain response of an assembly with sudden damage criterion ($a = 10$). From the figure it can be clearly observed that the pebble assembly with loose packing ($\eta = 0.626$) shows a compliant behaviour compared with the other two relatively densely packed assemblies (dotted and dashed curves). However, the critical stress seems to be independent of the packing factor although the onset strain depends on the packing factor. Also, the loosely packed assembly (solid line in Fig. 4b) shows a hardening behaviour similar to the case of gradual damage in Fig. 4b. Furthermore, the residual strain after unloading is large

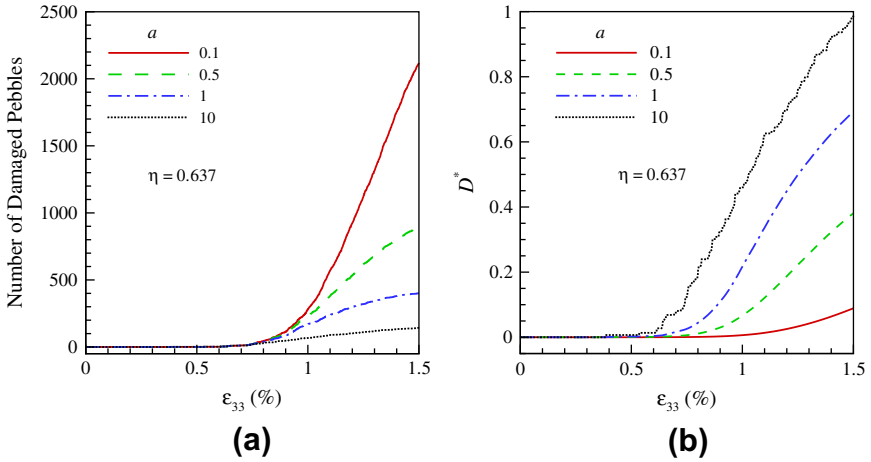

Fig. 5. (a) Number of damaged pebbles N_d (i.e., $D_i > 0$) as a function of applied strain; (b) average damage (D^*) of the assembly as a function of applied strain for different damage criteria for an assembly with $\eta = 0.637$.

for loosely packed assemblies for a given damage criterion as also observed in the previous studies [6,10]. Hence, in the present study, we observe a significant influence of the initial packing factor in addition to the influence of the damage coefficient in the unloading stage. This is relevant to the filling procedure of ceramic breeder pebbles in HCPB blankets to consider possible crushing of pebble and gap formation during and after the operations. It should be noted that in all the above simulations the spread of damage is not localized. In order to confirm that the non-localization of damage is not related to the non-uniform critical failure energy of the pebbles, one simulation with uniform critical failure energy ($\phi^{cr} = 8$ μJ) has been carried out showing a non-localized damage evolution (results not shown). The effect of non-localized damage is also evident from the insensitivity of the stress–strain response to different random distributions of the critical failure energy W_c (results not shown).

Fig. 5a shows the number of damaged pebbles N_d (i.e., pebbles with $D_i > 0$) for a pebble assembly with $\eta = 0.637$ plotted against the applied strain for different damage criteria. It can be observed that the total number of pebbles with $D_i > 0$ increases with decrease in the value of a. But, this can be mis-leading as the total damage level of the assembly need not necessarily be represented by this number. To gain a proper understanding of the total damage level of the assembly, we define another measure: "average damage" (D^*) for the assembly given by

$$D^* = \sum_{i=1}^{N} \frac{D_i}{N_d}, \tag{3}$$

where D_i is the damage value of pebble i and N_d is the number of pebbles with $D_i > 0$ as plotted in Fig. 5a. Thus the average damage-D^* represents the average percentage of damage accumulation in the pebbles with $D_i > 0$. Fig. 5b shows the average damage D^* plotted against the applied strain. Clearly, D^* increases with increase in the value of a. This means that the assembly with large D^* is more compliant than the assembly with small D^* directly explaining the large residual strain after unloading for the assembly with $a = 10$ as shown in Fig. 4a. Next, we analyse the effect of packing factor on the damage as a function of applied strain ϵ_{33} in Fig. 6. Fig. 6a shows that the number of damaged pebbles decreases with decrease in packing factor η at any given strain. But, the average damage D^* for different packing factors (see Fig. 6b) approaches the same value of unity at 1.5% strain explaining the convergence of stress–strain curves at the end of loading in Fig. 4b. However, the effect of packing factor is clearly visible through the residual strain after unloading. Here, the assembly with loose packing factor

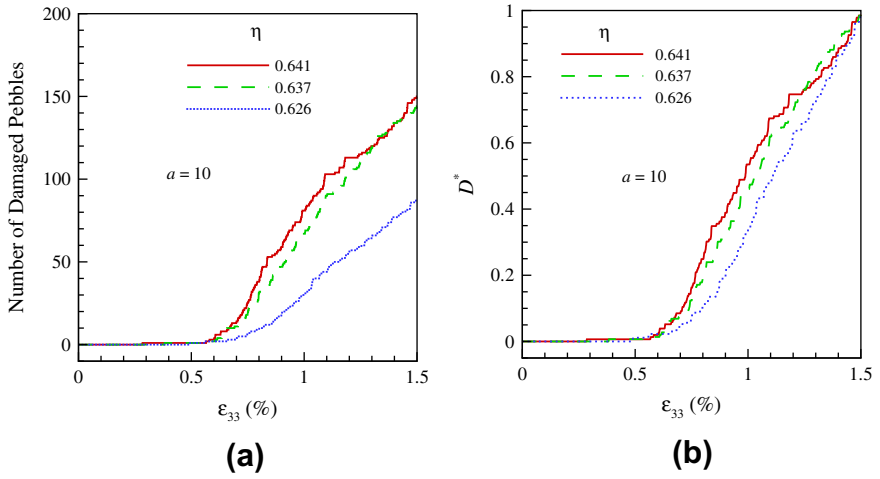

Fig. 6. (a) Number of damaged pebbles N_d (i.e., $D_i > 0$) as a function of applied strain; (b) average damage D^* in the assembly as a function of applied strain for different packing factors η for a given damage criterion $a = 10$.

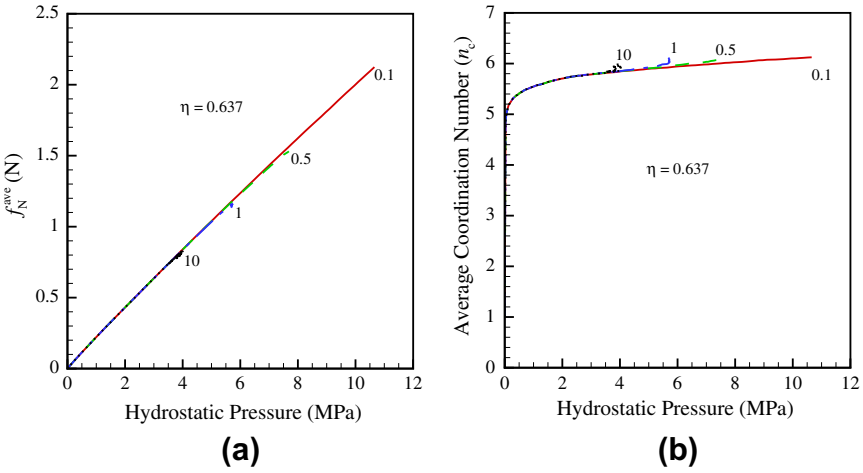

Fig. 7. (a) Average normal force (f_N^{ave}) and (b) average coordination number (n_c) as a function of hydrostatic pressure. The numbers in the figures refer to the value of damage coefficient a.

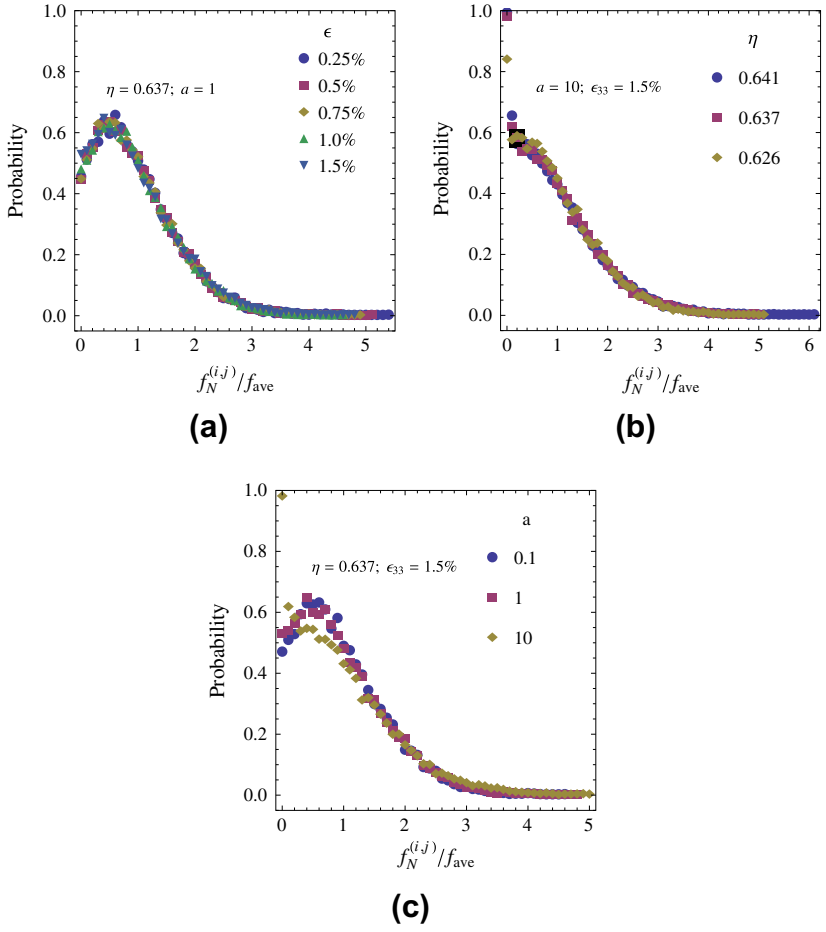

Fig. 8. Probability distribution of normalized normal contact force (a) at different strain levels for an assembly with $\eta = 0.637$ and $a = 1$; (b) for different packing factors η for a damage coefficient $a = 10$ and at $\epsilon_{33} = 1.5\%$; (c) for different damage coefficients with $\eta = 0.637$ at $\epsilon_{33} = 1.5\%$.

shows maximum residual strain after unloading despite having same damage level as the densely packed assemblies. Fig. 7a shows the evolution of average normal force (f_N^{ave}) as a function of hydrostatic pressure for different damage coefficients of the pebble assembly under investigation. Clearly, the average normal force is in direct correlation with the maximum stress shown in Fig. 4a. In addition, the average normal force is varying as a liner function of hydrostatic pressure as reported in previous studies [6,10]. Fig. 7b shows the evolution of coordination number as a function of hydrostatic pressure. Note the sudden rise in coordination number to 5 initially followed by a moderate rate of increase in coordination number. The sudden rise in the coordination number is due to the

fact that the initial coordination number of the assembly is very low (only one contact). Hence, a small initial load on the assembly brings it to the equilibrium coordination number. At this stage the assembly is closely packed resembling the experimental packing situation. Also, the average coordination number is only dependent on the overall hydrostatic state of the assembly rather than on the damage coefficient value. The effect of damage coefficient is to reduce the average contact force and hence the coordination number as is evident from the two (Fig. 7a and b).

We now investigate the probability distribution of normalized normal contact force between pebbles in the assembly similar to previous studies [6,11,12]. Fig. 8a shows the probability distribution of normalized normal contact force $(f_N^{(i,j)}/f_{\text{ave}})$ at different strain levels for an assembly with $\eta = 0.637$ and $a = 1$. Here, $f_N^{(i,j)}$ indicates the normal contact force exerted by pebble j on pebble i and f_{ave} is the average normal contact force on the assembly. At small strains the distribution shows a large tail and it starts to diminish with increase in strain. However, the distribution shows a unique shape at different strain levels despite a change in system compliance during loading. Similarly, the effect of packing factor η on the shape of the distribution for a given damage coefficient and strain is negligible (see Fig. 8b). Here also, the tail region decreases with increase in compliance level of the system similar to the case in Fig. 8a. The effect of damage coefficient on the probability distribution at the end of loading $(\epsilon_{33} = 1.5\%)$ is shown in Fig. 8c. The shape of the distribution is influenced by the damage coefficient considerably in the peak region than in the tail region although the shape can still be considered unique with a minor deviation. Here, the tail region increases with increase in the value of a albeit by a small amount. At first sight, this seems to be contradictory compared to the previous explanation based on compliance level of the system. But, in the case of a system with gradual damage (low a values) there will be more number of pebbles with $D_i > 0$ (see Fig. 5a) at the end of loading which reduces the maximum normalized normal contact force resulting in short tail. Here, the extent of the tail region is directly related to the number of pebbles already in the damage zone.

4. Conclusions

We have investigated the behaviour of a mono-sized pebble assembly under the uni-axial compression when the individual pebbles are allowed to fail. The results show that the stress–strain response of the granular assembly depends on the rate of damage (characterized by damage coefficient a) showing a clear transition from ideal plastic behaviour (in the case of sudden damage: $a = 10$) through a hardening behaviour (intermediate damage: $a = 1, 0.5$) to a non-linear stress–strain response (very slow damage or no-damage: $a = 0.1, 0$), conform Fig. 4a. It has been shown that the critical stress attained is influenced by the damage coefficient being employed; but the fraction of failed pebbles for the onset of critical stress is independent of damage coefficient. The critical stress is independent of packing factor although the strain at which the critical stress is attained depends on the packing factor (see Fig. 4b). The residual strain after unloading depends on the overall compliance of the assembly at the beginning of unloading step. The average damage D^* is used to characterize the damage level of the assembly with a reasonable accuracy rather than with the number of damaged pebbles N_d. With increase in value of a the average damage D^* also increases indicating an increase in compliance level. This observation is reinforced by the observation of increase in residual strain after unloading with increase in a (compare Figs. 4a and 5b). However, the D^* values for assemblies with different packing factors for a given damage criterion converges to a single value. Hence, the difference in residual strain after unloading in these systems is attributed to the difference in packing factors, see Figs. 4b and 6b.

It should be noted that the present analysis is based on a continuum damage evolution scheme which may not represent the behaviour of granular systems under compressive stress in full detail. The breeder material (Lithium Orthosilicate) for fusion reactors being brittle resembles a sudden damage failure. A gradual damage criterion may be more appropriate for systems such as electrode materials used in fuel cells and neutron multiplier materials (Beryllium) in fusion reactors. In view of the little knowledge about the damage mechanisms in these individual systems, the present analysis helps us to gain a preliminary insight into their behaviour as granular assemblies in a qualitative manner. Furthermore, the present paper highlights the behaviour of the assemblies with different damage criteria and different packing factors. The methodology presented in this paper can also be extended to investigate the thermomechanical effects of crushable pebble assemblies without any limitations.

Acknowledgments

This work supported by the European communities under the contract of Association between EURATOM and Karlsruhe Institute of Technology (KIT) was carried out within the framework of the European Fusion Development Agreement. The views and opinions expressed herein do not necessarily reflect those of the European Commission. The authors thank R. Knitter and R. Rolli for providing the crush load data for Orthosilicate Pebbles.

References

[1] L. Boccaccini, J.-F. Salavy, O. Bede, H. Neuberger, I. Ricapito, P. Sardain, L. Sedano, K. Splichal, Fusion Engineering and Design 84 (2009) 333–337.
[2] S. Zhao, Multiscale Modeling of Thermomechanical Properties of Ceramic Pebbles, Ph.D. thesis, Karlsruhe Institute of Technology, 2010. <http://digbib.ubka.uni-karlsruhe.de/volltexte/1000021237>.
[3] S. Zhao, Y. Gan, M. Kamlah, T. Kennerknecht, R. Rolli, Engineering Fracture Mechanics. http://dx.doi.org/10.1016/j.engfracmech.2012.05.011.
[4] O. Ben-Nun, I. Einav, A. Tordesillas, Physical Review Letters 104 (2010) 108001.
[5] W. Dienst, H. Zimmermann, Journal of Nuclear Materials 155–157 (1988) 476–479.
[6] Y. Gan, M. Kamlah, Journal of the Mechanics and Physics of Solids 58 (2010) 129–144.
[7] W.S. Jodrey, E.M. Tory, Physical Review A 32 (1985) 2347–2351.
[8] Y. Gan, M. Kamlah, J. Reimann, Fusion Engineering and Design 85 (2010) 1782–1787.
[9] A. Ying, J. Reimann, L. Boccaccini, M. Enoeda, M. Kamlah, R. Knitter, Y. Gan, J. van der Laan, L. Magielsen, P. Maio, G. Dell'Orco, R.K. Annabattula, J. Van Lew, H. Tanigawa, S. van Til, Fusion Engineering and Design. http://dx.doi.org/10.1016/j.fusengdes.2012.02.090.
[10] R.K. Annabattula, Y. Gan, M. Kamlah, Fusion Engineering and Design. http://dx.doi.org/10.1016/j.fusengdes.2012.02.033.
[11] Z. An, A. Ying, M. Abdou, Fusion Engineering and Design 82 (2007) 2233–2238.
[12] Y. Gan, M. Kamlah, H. Riesch-Oppermann, R. Rolli, P. Liu, Crush probability analysis of ceramic breeder pebble beds under mechanical stresses, Journal of Nuclear Materials 417 (2011) 706–709.